2026 IEEE International Conference on Robotics and Automation (ICRA 2026)
June 1-5, 2026. Vienna, Austria

A Non-Invasive Closed-Loop Myoelectric Prosthetic Hand Featuring Electrotactile Sensory Feedback

Guanyu Zhu[1], Yilong Dou[1], Qiong Wu[1], and Qichuan Ding[2]

Abstract— **The absence of sensory feedback has been a critical challenge for myoelectric prostheses in recent years. While electrotactile feedback has emerged as an effective non-invasive solution, significant challenges remain in simultaneously ensuring real-time performance, processing EMG signals under electrical stimulation interference, and transmitting richer sensory information. This study proposes a multidimensional bio-inspired electrical stimulation feedback paradigm, implemented on a self-developed closed-loop myoelectric prosthetic hand system with real-time interference avoidance capability. Utilizing the human cutaneous nervous system as the feedback pathway, our paradigm establishes diverse electrotactile patterns through real-time modulation of four-channel stimulation parameters (frequency and current intensity). Experimental results with both able-bodied participants and amputees demonstrate that the proposed paradigm can accurately convey prosthetic state information, enabling users to perceive object size, length, shape, and stiffness through the prosthetic hand. This feedback framework provides a viable sensory restoration solution for prosthetic applications.**

I. INTRODUCTION

Recent years have witnessed remarkable progress in intelligent prosthetic hand research, with the primary objective of restoring lost hand functions for upper-limb amputees to significantly improve their quality of life and autonomy. Surface electromyography (sEMG)-controlled prostheses have become a focal research direction with advancing technologies.

A critical limitation in current prosthetic usage is the lack of ”embodiment” [1]–[3] - the perceptual experience where users naturally integrate the prosthesis as part of their body. When users must consciously control the device or visually monitor every movement, the prosthesis remains merely an external tool requiring strenuous operation [4]–[6]. This embodiment deficit severely limits practical utility and user experience, stemming from two fundamental issues: (1) The dissociation between control and feedback in most open-loop prosthetic systems forces heavy reliance on visual feedback, resulting in high cognitive load and unnatural operation; (2) Existing sensory feedback methods remain inadequate in information richness, naturalness, and long-term stability for accurately conveying force, angle, and position information. Therefore, a closed-loop system simultaneously encoding these multidimensional mechanical signals through artificial electrical stimulation mimicking neural coding patterns is essential for embodiment restoration.

Among various feedback approaches, electrical stimulation feedback has gained attention due to its low energy consumption, programmability, and compact size [7]. This method bypasses biological receptors to directly stimulate peripheral nerves, transmitting information through natural neural pathways to reduce cognitive load and visual dependence. It enables precise grasp force perception, thereby enhancing control capability and facilitating embodiment [8]–[12]. Electrical stimulation interfaces can be either invasive or non-invasive, with the latter being more widely adopted in prosthetic feedback systems due to higher safety, lower cost, and better user acceptance. However, current electrotactile feedback still suffers from low resolution, interference, and limited information bandwidth [13]–[15].

The muscle spindle, as the primary proprioceptive organ encoding muscle length and velocity changes, provides biological inspiration for prosthetic embodiment restoration [16]. Some studies have implemented muscle spindle-inspired models in prosthetics through biomimetic algorithms [17]. Building upon electrical stimulation feedback models targeting muscle receptors, we developed a novel feedback paradigm incorporating current intensity modulation to enrich sensory information dimensions and enhance prosthetic feedback capability.

To validate our approach, we designed a real-time multichannel electrical stimulation closed-loop myoelectric hand system. Experiments with four participants (including one forearm amputee) demonstrated that our paradigm can accurately convey prosthetic joint angles and force information, enabling users to discriminate object size, length, shape, and stiffness - confirming the feasibility of our approach for enhanced motor-sensory feedback. The main contributions of this paper are summarized as follows:

1) Development of a multidimensional electrical stimulation feedback paradigm incorporating a muscle spindle-inspired algorithm. This framework independently modulates multichannel stimulation parameters (amplitude and frequency) based on neural discharge models to provide real-time feedback of individual finger angles and forces.
2) Implementation of a real-time multichannel closed-loop

This work was supported in part by the National Natural Science Foundation of China under Grant 62373086, by the Liaoning Province Applied Basic Research Program(2025JH2/101330131), by the Guangdong Basic and Applied Basic Research under 2023A1515140014, and by the State Key Laboratory of Robotics under Grant 2024-O14.(Corresponding authors: Qichuan Ding.)

[1]G. Zhu, Q. Wu and Y. Dou are with the Faculty of Robot Science and Engineering, Northeastern University, Shenyang 110169, China (e-mail: zhugy1@mails.neu.edu.cn).

[2]Q. Ding is with the Faculty of Robot Science and Engineering, Northeastern University, Shenyang 110169, China, and also with the Foshan Graduate School of Innovation, Northeastern University, Foshan 528311, China (e-mail: dingqichuan@mail.neu.edu.cn).

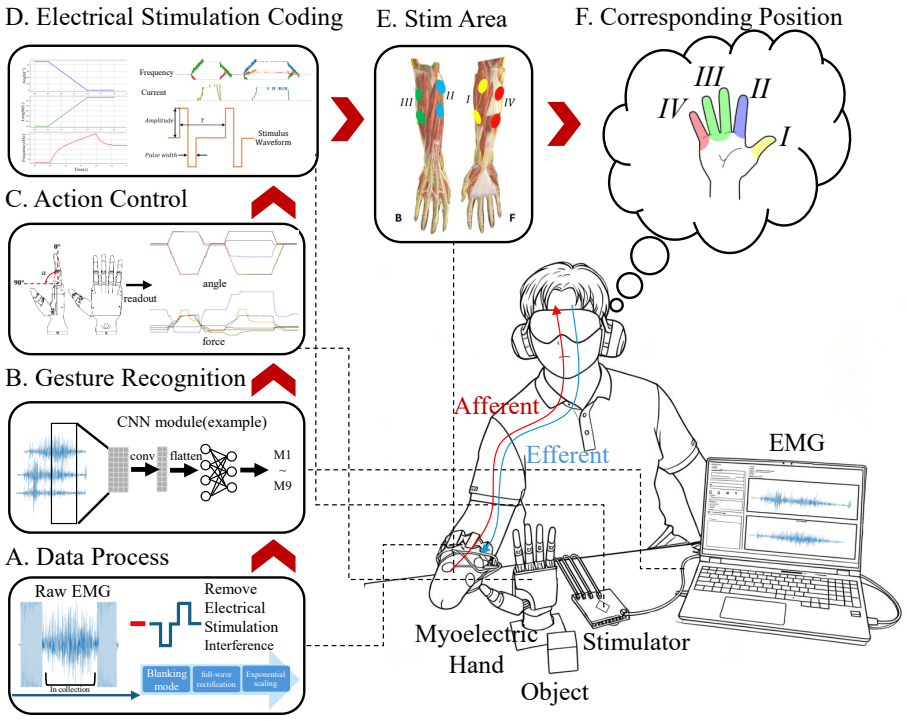

Fig. 1. Overview of the Closed-Loop Myoelectric Prosthetic Hand System. An individual with transradial amputation controls a prosthetic hand to grasp and perceive objects by wearing a myoelectric bracelet paired with four sets of surface electrodes.(A) Electromyographic (EMG) signals are collected via the bracelet, processed using a blanking method to remove electrical interference, and then rectified and scaled.(B) A Convolutional Neural Network (CNN) model performs gesture recognition based on the EMG signals.(C) Upon gesture identification, the prosthetic hand executes the corresponding movement and transmits signals from angle and force sensors to an electrical stimulator.(D) The stimulator employs a biomimetic algorithm to compute frequency and current intensity, converting them into bidirectional electrical stimulation pulses.(E) These electrical pulses are delivered through the cutaneous nervous system of the forearm to the brain's sensory cortex.(F) By interpreting the stimulation, the user perceives tactile feedback corresponding to specific fingers.

myoelectric hand system comprising an EMG bracelet, prosthetic hand, stimulator, and surface electrodes. The system acquires EMG signals for gesture recognition and prosthetic control while delivering electrical stimulation feedback corresponding to finger kinematics and kinetics. Experimental validation demonstrates the paradigm's advantages in environmental perception.

II. METHODOLOGY

A. Closed-Loop Feedback System Overall Architecture

The comprehensive workflow of the closed-loop myoelectric prosthetic hand system encompasses data acquisition, signal processing, pattern recognition, motion control, and electrical stimulation feedback control. First, the eight-channel EMG signals S_1–S_8 collected by the MYO armband undergo decoding and filtering(Fig. 1A). A blanking method is applied to separate collected samples from stimulation artifacts, ensuring only EMG signals unaffected by electrical stimulation are retained.Next, a CNN [18] extracts the activation levels of motor units across different channels to determine the intended motion pattern M_1–M_9(Fig. 1B). Based on the identified motion pattern M, commands are transmitted via RS232 serial communication to drive the actuators of the prosthetic hand. Simultaneously, angle and force data from the prosthetic hand are read for feedback(Fig. 1C). The acquired prosthetic hand data are then fed into a muscle spindle biomimetic control algorithm, which computes the current amplitude I and stimulation frequency F of electrical pulses(Fig. 1D). These pulses are delivered through four pairs of circular dry electrodes to provide electrotactile feedback to the user(Fig. 1E). Finally, by interpreting spatially distributed electrical stimulation, the user perceives the state of individual fingers, enabling them to plan movements and complete the closed-loop control cycle(Fig. 1F).

B. EMG Signal Recording and Processing

The EMG signals were measured using a MYO armband (sampling frequency of 200 Hz), acquiring raw data without hardware filtering. Since the multi-channel time-varying electrical stimulation signals can severely interfere with the EMG signals and become mixed with the valid signals, they are difficult to remove individually. This system employs the blanking method to separate stimulation and EMG signals in a time-division manner [19], dividing the EMG signals into two states: acquisition and stimulation. During the stimulation phase, electrical stimulation is activated while the EMG signals contaminated with artifacts are discarded, and the hand gesture remains fixed without changes. In the acquisition state, electrical stimulation is stopped, and the collected EMG signals are retained. The majority voting algorithm is then used to determine the hand gesture to be maintained in the next stimulation phase. The timing diagram of this process is shown in Fig. 2. The green line indicates

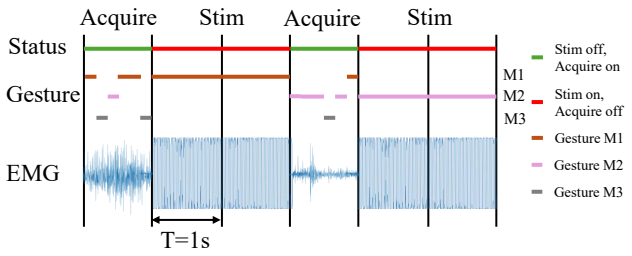

Fig. 2. Timing diagram of the acquisition-stimulation-acquisition paradigm, including the acquisition state, hand gestures (M1–M3), and EMG signals.

that the stimulation is deactivated and EMG acquisition is enabled, whereas the red line shows that the stimulation is activated and acquisition is disabled. Meanwhile, the brown, pink, and gray lines represent the execution of gestures M1, M2, and M3, respectively. The acquired EMG data is stored, maintaining the most recent set of collected data, and undergoes full-wave rectification and exponential scaling.

C. Pattern Recognition

Since the stimulation-acquisition-stimulation pattern adopted in this system results in discretized EMG signals, we consequently selected discrete gesture recognition tasks as the control objective. For gesture recognition tasks, CNN architectures demonstrate tremendous potential [20].A typical CNN model consists of convolutional layers, pooling layers, activation functions, and fully connected layers. In this study, we constructed a CNN model based on the architecture described in [18], maintaining an identical structure that exhibits multi-scale, cross-temporal, and cross-channel characteristics.

D. Stimulation method

For multi-channel close-range electrical stimulation, electrical interference is inevitable. Therefore, the key challenge lies in minimizing its impact on data while ensuring the effectiveness of electrotactile stimulation. From the perspective of electrotactile stimulation, continuous electrical stimulation allows the human body to perceive changes in current and frequency more distinctly, and multi-channel stimulation can provide richer information. However, such stimulation introduces significant interference with EMG signals. Conversely, from the standpoint of reducing electrical interference, single-point, fixed, and brief electrical stimulation facilitates the use of fixed filters for noise removal. However, the information conveyed through electrotactile stimulation in this manner is highly limited. To strike a balance, we adopt a compromise solution: employing multi-channel, dynamic, and short-duration square-wave pulses as the stimulation source.

Although some amputees retain intact nerve endings in their residual limbs, enabling feedback similar to that of natural fingers, others cannot stimulate the phantom finger map (PFM) [21] region due to nerve damage at the amputation site, varying recovery states, or the limited penetration depth of transcutaneous electrical nerve stimulation (TENS). Thus,

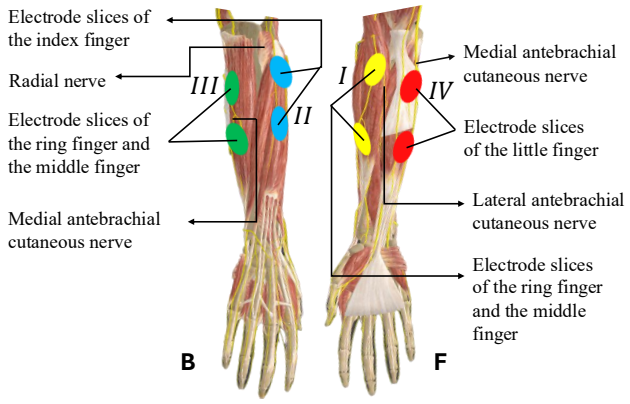

Fig. 3. The corresponding positions of four pairs of electrical stimulation electrodes on the right arm and their respective stimulated nerves.

this study targets intact nerves in the forearm [22], [23], including the medial antebrachial cutaneous nerve, lateral antebrachial cutaneous nerve, and portions of the radial nerve. The electrode placement is illustrated in Fig. 3, with electrodes of the same color representing a pair.

E. Feedback Algorithm

The myoelectric prosthetic hand employed in this study features six degrees of freedom (DOF) and six force sensors. It transmits data to a computer via the RS232 protocol using a serial connection. The six DOFs of the prosthetic hand were mapped to four stimulation channels using a grouping strategy: the two thumb DOFs were averaged and assigned to CH1; the index finger to CH2; the middle and ring fingers (averaged) to CH3; and the little finger to CH4. Additionally, building upon previous research on the muscle spindle model [17], we adjusted the transfer function based on the actual sampling frequency to establish the relationship between frequency and joint angle. By modulating the frequency and current intensity, we conveyed information corresponding to each DOF, including a mean-value calculation for two-DOF mappings. The formula is as follows:

$$H(z) = \frac{L_i}{F_i} = \frac{6.961 - 5.686z^{-1} - 0.863z^{-2}}{1 - 0.685z^{-1} + 0.001z^{-2}} \tag{1}$$

$$\begin{aligned} f_i[n] = {} & 0.685 f_i[n-1] - 0.001 f_i[n-2] + 6.961 L_i[n] \\ & - 5.686 L_i[n-1] - 0.863 L_i[n-2] \end{aligned} \tag{2}$$

$$L_i = 0.02745 A_i + 1.08 \tag{3}$$

Here, Equation (1) represents the z-domain transfer function of the muscle spindle model, Equation (2) is the difference equation derived from the transformed transfer function, and Equation (3) describes the conversion formula between muscle fiber length (L) and joint angle (A) in the muscle spindle model. F denotes the discharge frequency, while i indicates the corresponding electrical stimulation channel. Based on these, we obtained the conversion formula between the prosthetic finger angle and stimulation frequency. The

TABLE I
DETAILS OF FOUR SUBJECTS

Subject	Age	Sex	Weight	Height	Dominant hand	Amputation situation	Cause	Year since amputation	Own prosthesis	Utility Frequency (Day)	Myoelectric prosthesis experience
S1	53	M	65	171	R	Left, remain forearm length is about 20.1cm	Trauma	3	Functionality	<2 hour	None
S2	24	M	110	186	R	/	/	/	/	/	/
S3	21	M	63	178	R	/	/	/	/	/	/
S4	24	M	70	175	R	/	/	/	/	/	/

current intensity was calculated according to the following formula:

$$I_i = I_{i,\min} + (I_{i,\max} - I_{i,\min}) \cdot F_i^2 \tag{4}$$

Where I represents the discharge current, $I_{i,\min}$ denotes the minimum perceptible threshold current for each electrical stimulation channel, and $I_{i,\max}$ corresponds to the pain threshold current of the respective channel. F is the normalized value of the force exerted on the prosthetic finger. Due to slight residual readings from the myoelectric prosthetic hand even in non-contact states—and its rapid increase upon force application—a quadratic function was employed to reduce perception during non-contact conditions while enhancing force sensitivity during grasping.

III. EXPERIMENT

A. Human Subjects Recruitment

Three healthy participants (all male, mean age 23.0 ± 1.4 years) and one male amputee (aged 53 years) were recruited for our experiment. Detailed demographic information of participants is presented in Table I. Prior to participation, all subjects were informed of the experimental procedures and provided written informed consent. All ethical and experimental procedures and protocols were approved by the relevant review committees, and the experiments were conducted in compliance with applicable guidelines and regulations while adhering to the approved protocols.

B. Experimental Setup

In the experiments, the MYO EMG armband (Thalmic Labs, Canada) was employed to record eight-channel EMG signals using eight medical-grade stainless steel monopolar differential electrodes. The EMG data were transmitted via Bluetooth to a computer running the connection program with 8-bit signed resolution, and a CNN model was utilized to recognize the current gesture, outputting the results to the control board. The control chip (STM32F103, @STMicroelectronics, Switzerland) transmitted signals to the dexterous five-fingered anthropomorphic hand (RH56DFX, @InspireRobots, China) for movement, while simultaneously receiving angle and force feedback from the hand. Based on this information, the control chip regulated the electrical stimulator (ENS001-A, @Nanochap, China) to generate four-channel electrical stimulation with varying currents (0–25 mA) and frequencies (10–200 Hz), which was then delivered through four pairs of medical-grade nonwoven dry electrode patches (25×25 mm, circular).

For all experiments, the MYO armband was worn below the elbow, with the first electrode positioned at the humeroulnar joint, following the single-MYO configuration in the Ninapro DB5 dataset. For amputees, the four pairs of stimulation electrodes were placed in the corresponding PFM regions to provide tactile feedback for different fingers (CH1 for the thumb's two DOF, CH2 for the index finger's one DOF, CH3 for the middle and ring fingers' two DOF, and CH4 for the little finger's one DOF). For able-bodied participants, one end of the electrodes was arranged around the arm near the wrist, avoiding major nerves, while the other end was placed on the corresponding fingertips. Before electrode and armband placement, all skin areas were cleaned with alcohol, and the electrodes were secured with medical tape to prevent detachment. The stimulation pulse width was fixed at 0.1 ms. In Experiments 2 and 3, participants wore blindfolds and noise-canceling ear protection to eliminate visual and auditory feedback.

Prior to the formal experiments, individualized stimulation intensity was determined for each participant to ensure safety, with perceptual and discomfort thresholds recorded. A fixed pulse width (0.1 ms) and the lowest frequency (10 Hz) were initially set, and the current intensity was gradually increased from 0 in increments of 0.1 mA. The point at which the participant first perceived tactile sensation was recorded as the preliminary perceptual threshold. Subsequently, the current was further increased in 0.1 mA steps until the participant reported pain, yielding a preliminary discomfort threshold. This process was repeated three times, and the average values were taken as the final perceptual and discomfort thresholds. At the discomfort threshold, the frequency was incrementally raised to the maximum setting (200 Hz). If pain was reported during this process, the discomfort threshold was adjusted downward, and the pulse width was modified if necessary.

C. Experiment 1: Gesture Recognition

Experiment 1 aimed to verify whether the proposed model could accurately estimate motion intention under stimulation conditions. The experiment was developed as an improvement upon the method described in [24]. All participants (1 amputee and 3 able-bodied individuals) participated in Experiment 1. In this experiment, participants were required to perform the following hand gestures: thumb extension,

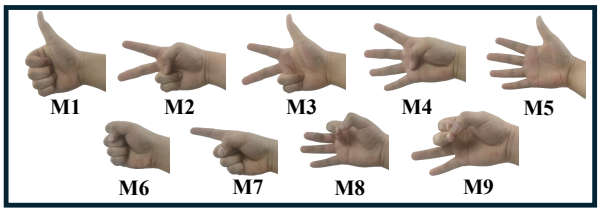

Fig. 4. Nine gestures used for motion recognition, where M1 to M9 represent the gesture identification codes.

index and middle finger extension with other fingers flexed, ring and little finger flexion with other fingers extended, thumb pressing against the base of the little finger, five-finger extension, five-finger grasp, index finger extension, two-finger (thumb-index) pinch grasp, and three-finger (thumb-index/middle) pinch grasp, as shown in Fig. 4. All participants sat comfortably at a table with their elbows resting on the surface, their upper arms naturally extended, and their palms facing upward. They performed the specified gestures sequentially based on prompts displayed on a computer screen. In each session, participants repeated each gesture 6 times, holding it for 5 seconds with 5-second rest intervals between repetitions and 10-second rest intervals between different gestures. Participants repeated the experiment 3 times, with 5-minute breaks between sessions to avoid muscle fatigue. All collected trial data were divided into training and test sets at an 80%/20% ratio, and electrical stimulation was kept inactive during the experiment.

After data collection, participants rested before proceeding to the actual validation phase. The program randomly prompted participants to perform one of the nine gestures for 5 seconds, with 5-second intervals between prompts. Each gesture appeared 5 times. The validation test was conducted twice, divided into a stimulation group and a non-stimulation group, with a 5-minute rest between groups. Participants wore ear coverings and performed the gestures without any feedback other than electrical stimulation. The program recorded the executed gesture during each sampling and compared it with the intended gesture. The accuracy rate was converted into a precision score as the final result. This metric reflects the control accuracy, real-time performance, and stability of the prosthetic hand.

D. Experiment 2: Motion Perception Experiment

Experiment 2 aimed to evaluate whether the proposed electrical stimulation feedback system could accurately convey finger angle and force information of the prosthetic hand. All participants (1 amputee and 3 able-bodied individuals) participated in Experiment 2. In this experiment, participants underwent a 10-minute training session to familiarize themselves with the electrical stimulation feedback for different gestures. Subsequently, they wore earplugs and blindfolds and sat on a chair, relying solely on four-channel electrical stimulation to identify the currently executed gesture. The prosthetic hand was fixed on a table, and an operator randomly manipulated it to perform the 9 gestures from Experiment 1, with each gesture repeated 4 times (totaling 36 trials). The operator did not guide or influence the participants' recognition strategies or results. The executed gestures, participant feedback, and reaction times were recorded. Reaction time was defined as the duration from when the prosthetic hand completed the gesture change to when the participant reported the perceived gesture.

E. Experiment 3: Object Grasping Recognition Experiment

Experiment 3 aimed to evaluate the effectiveness of the proposed muscle spindle-inspired feedback model in distinguishing object shape, size, length, and stiffness. This experiment was developed as an improvement upon the method described in [21]. Only participants S2 and S3 participated in Experiment 3 due to scheduling constraints for the others. The experiment consisted of three tasks: size and length perception, shape perception, and softness perception. The participant and setup configurations remained the same as in Experiment 2.

For size and length perception, three cylinders of identical length (10 cm) but differing diameters (50 mm [large], 40 mm [medium], and 30 mm [small]) were used. Different lengths were simulated by inserting the cylinders from the little finger side at varying distances (8 cm [four-finger length], 6 cm [three-finger length], and 2 cm [one-finger length]), creating 9 conditions. In the shape perception task, a cube, sphere, and cylinder with equal side lengths/diameters (40 mm) were used. For softness perception, cotton and wooden spheres with diameters of 30 mm were employed.

Before each task, participants were given 5 minutes to familiarize themselves with the objects. The operator then randomly placed the objects within the prosthetic hand's grasping range, and the hand was controlled to grasp them. Task 1 involved 4 trials per condition, Task 2 involved 5 trials per object, and Task 3 involved 10 trials per object. The executed actions, participant feedback, and reaction times were recorded. Reaction time was defined as the duration from when the prosthetic hand contacted the object to when the participant reported the perceived object type.

IV. RESULTS AND DISCUSSION

A. Determination of Electrical Stimulation Parameter Thresholds

We measured the perceptual and discomfort thresholds for all four subjects and established the baseline stimulation intensity for each individual (Table II). The perceptual thresholds of healthy subjects were generally lower than those of amputees, except for S4. Notably, S4—who had exercise records within 24 hours—exhibited a perceptual threshold closer to that of amputees, along with a lower discomfort threshold compared to healthy subjects. This suggests that reduced muscle mass or muscle fatigue may lead to an increase in perceptual thresholds. Regarding discomfort thresholds, S2 exhibited the highest threshold, followed by S1. Considering that S2 had a higher body weight and S1 had less forearm muscle mass than healthy subjects, while S4 maintained sufficient muscle mass and low body fat, we infer that fat content at the stimulation site plays a role. Fat may

TABLE II

PERCEPTION THRESHOLDS, DISCOMFORT THRESHOLDS, AND BASELINE STIMULATION INTENSITIES IN FOUR-CHANNEL ELECTRICAL STIMULATION

Subject	Perception Threshold (mA)	Discomfort Threshold (mA)	Baseline Intensity (mA)
S1*	1.3, 1.8, 0.7, 0.6	18.7, 19.6, 20.4, 17.9	2.4, 5.3, 5.5, 3.6
S2	0.6, 0.4, 0.4, 0.5	21.3, 22.5, 23.4, 20.8	2.1, 2.8, 2.0, 2.5
S3	0.8, 0.6, 0.9, 0.6	15.6, 16.4, 18.3, 15.8	1.8, 2.5, 1.8, 1.3
S4	1.9, 1.9, 1.6, 0.5	12.5, 7.4, 12.5, 22.0	3.5, 2.5, 2.0, 3.0

* indicates amputated subject.

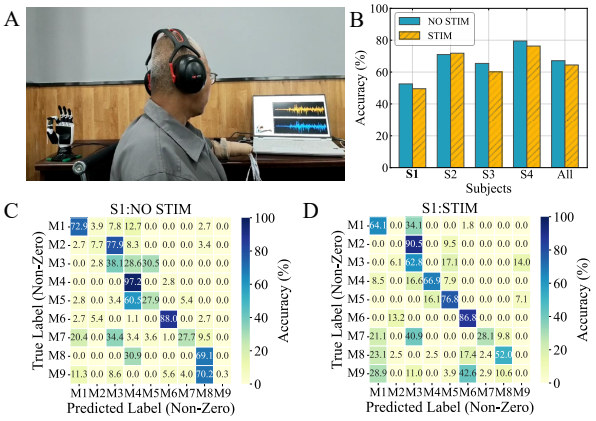

Fig. 5. Gesture Recognition Task. (A) Experimental setup. Participants wearing earmuffs performed gestures following on-screen prompts under conditions with/without electrical stimulation. The prosthetic hand was placed outside their field of vision as a reference for the current action.(B) Gesture recognition accuracy of four participants under both conditions.(C)(D) Confusion matrices for different gestures performed by amputee S1 under no electrical stimulation and electrical stimulation conditions, respectively.

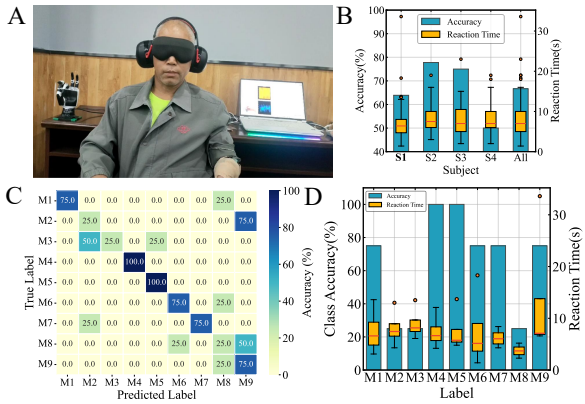

Fig. 6. Motion Perception Task. (A) Experimental setup. The operator randomly selected gestures from M1 to M9 to control the prosthetic hand. Participants were required to wear earplugs and an eye mask, relying solely on electrical stimulation feedback to identify the current prosthetic hand motion.(B) Distribution of average accuracy and reaction time for the four participants in the motion perception task. (C) Confusion matrix for the accuracy of gesture perception by the amputee in the motion perception task. (D) Distribution of recognition accuracy and reaction time for different gestures by the amputee in the perception task.

provide greater impedance [25], protecting nerves during stimulation.The baseline stimulation intensity—defined as the current level at which subjects could easily perceive changes in electrical stimulation—varied among the four participants. The amputee (S1) and the fatigued subject (S4) had similar baseline values, while S2 (with higher fat content) required a higher baseline than the normal subject (S3). This suggests that baseline stimulation intensity may be inversely proportional to muscle mass but positively correlated with muscle state and fat content.

B. Gesture Recognition Task

Fig. 5(B) presents the classification accuracy rates of nine gestures (excluding the relaxation state) performed by participants under both activated and deactivated electrical stimulation conditions in a real-time gesture recognition task. Without stimulation, the amputee achieved an accuracy of 52.56%, while healthy participants attained an average accuracy of 71.98%, yielding an overall mean accuracy of 67.12%. Under stimulation, the amputee's accuracy was 49.55%, healthy participants averaged 69.43%, and the collective mean was 64.46%. It can be observed that due to time-division processing reducing interference from electrical stimulation, real-time performance degradation led to slightly lower results. However, the majority voting method prevented a significant drop in precision, even showing slight improvement in S2's outcomes.

Fig. 5(C,D) displays the confusion matrices of gesture classification results for the amputee under both conditions. We observed substantial deviations when the amputee attempted to perform M2 and M9 gestures. Specifically, M2 was frequently misclassified as M3, and M9 was confused with M8, indicating difficulties in controlling thumb and middle finger movements. Poor thumb dexterity also negatively affected the performance of M3, M5, and M7. With electrical stimulation, the majority voting algorithm and motion stabilization techniques partially mitigated misclassifications for M3 and M5, helping maintain correct labeling. This experiment demonstrates that the closed-loop electrical stimulation prosthetic hand control system not only avoids interference with EMG signals but also retains a certain degree of maneuverability. Moreover, it assists users in stabilizing movements, thereby enhancing usability.

C. Motion Perception Task

Fig. 6(B) presents the recognition accuracy and reaction time of participants in the motion perception experiment. Among them, S1 (an amputee) achieved a recognition accuracy of 63.89%, while the three healthy participants attained accuracies of 77.78%, 75%, and 50%, respectively, with an overall average accuracy of 66.67%. The reaction times of all four participants primarily ranged between 5–10 seconds, with the amputee responding faster. This may be attributed to long-term adaptation to sensory substitution strategies in daily life, resulting in enhanced sensitivity to artificial feedback cues. Additionally, the absence of conflicting natural

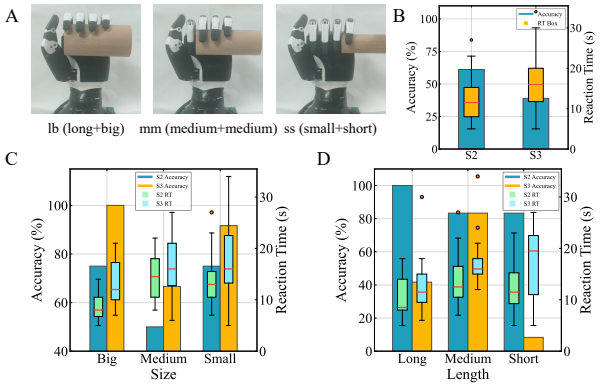

Fig. 7. Dual-Factor Object Grasping Recognition Task (Size & Length).(A) Three out of nine object placement conditions: large + long, medium + medium length, small + short.(B) Recorded average accuracy and reaction time for two participants in the grasping recognition task. (C) Accuracy and reaction time records for object size discrimination.(D) Accuracy and reaction time records for object length discrimination.

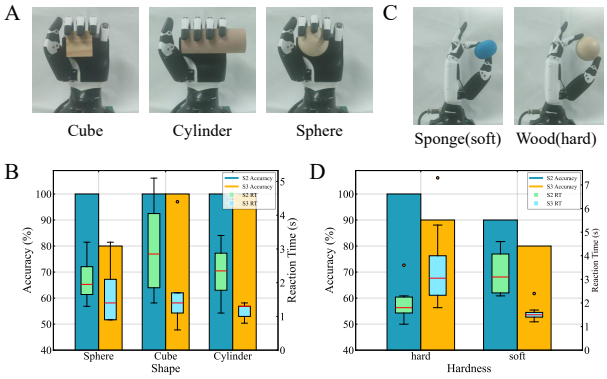

Fig. 8. Single-Factor Object Grasping Recognition Task (Shape & Stiffness).(A) Three types of objects to be grasped.(B) Recognition accuracy and reaction time for two participants in identifying the three object shapes.(C) Hand gestures and grasping postures of the prosthetic hand when gripping spheres of different materials.(D) Recognition accuracy and reaction time for two participants in discriminating objects with varying stiffness levels.

proprioceptive input may reduce sensory integration time. Notably, healthy participant S4 exhibited weaker perceptual ability. Post-experiment inquiry revealed that S4 had engaged in arm movements within the past 24 hours and reported insensitivity to electrical stimulation during the adaptation phase, along with slower learning of stimulation patterns. Excluding S4, the other two healthy participants demonstrated higher perceptual accuracy than the amputee.

Fig. 6(C,D) displays the recognition accuracy and reaction time of the amputee for the nine gestures. Performance was notably weaker for M2, M3, and M8, while M9 required a longer reaction time. According to participant feedback, M2 and M3, as well as M8 and M9, had similar gesture patterns, and the averaged electrical stimulation feedback for the middle and ring fingers made them harder to distinguish. This experiment demonstrates that multichannel electrical stimulation combined with a muscle spindle model for frequency computation can effectively convey prosthetic hand angle information through neural pathways. However, the method requires a learning period and is susceptible to variations in physical and muscular states.

D. Object Grasping Recognition Task

Fig. 7(B) presents the accuracy rates (61.11% for S2 and 38.89% for S3) and median reaction times (11.5s and 16s, respectively) for two participants simultaneously perceiving object size and length, while Fig. 7(C,D) show their performance in separate size and length discrimination tasks. In size recognition, S2 achieved accuracies of 75% (large), 50% (medium), and 75% (small) with median reaction times of 8s, 14.5s and 13s, whereas S3 showed higher accuracies (100%, 75%, and 91.67%) but longer reaction times (12s, 16s, and 16s). For length discrimination, S2 maintained consistently high accuracy (100%, 83.33%, and 83.33%) with reaction times of 8.5s, 11.5s and 12.5s, while S3 exhibited greater variability (41.67%, 83.33%, and 8.33%) and significantly longer reaction times (11.5s, 16s, and 19.5s). Notably, S2 demonstrated superior length recognition but poorer size discrimination, with the opposite pattern observed for S3. Analysis of grasping kinematics revealed that object size perception primarily correlated with grip force and angle adjustments, whereas length discrimination depended more on stimulation channel selection, suggesting distinct neural processing mechanisms for different stimulus dimensions. Furthermore, lower recognition accuracy was generally associated with prolonged reaction times and increased response variability, likely reflecting greater task difficulty or uncertainty in sensory discrimination.

Fig. 8(B) shows high shape recognition performance, with only one error by S3 (80% accuracy), while all other judgments were correct. Reaction times were generally within 2–4 s, with S3 responding faster. Fig. 8(C,D) further demonstrate reliable stiffness discrimination. Accuracy ranged from 80% to 100% across participants (S2: 100%/90%; S3: 90%/80% for soft/hard), with median reaction times below 3.5 s.

The results demonstrate that under single-factor experimental conditions, judgment accuracy is significantly higher than in dual-factor experiments. Compared with the single-factor baseline experiments in reference [21], the proposed feedback method enables more stable and accurate identification of single-factor variation conditions while maintaining satisfactory performance in dual-factor experiments, with the added capability of recognizing a greater variety of object information.

In conclusion, the experiments demonstrate that the multichannel biomimetic electrical stimulation system adopted in this study can rapidly and comparatively identify object characteristics including shape, size, length, and hardness without requiring additional informational cues. This approach provides users with rich information while enabling simultaneous recognition of multiple attributes. However, as the number of information types being perceived increases, the recognition accuracy decreases accordingly, and response times become prolonged.

This study involved a limited number of subjects (one

amputee and three able-bodied participants), and the object grasping task was conducted with two participants. The results therefore serve as proof-of-concept validation under controlled laboratory conditions. Future work will include larger-scale amputee studies and fully wearable experiments to evaluate long-term usability.

V. CONCLUSIONS

In summary, this study developed a multidimensional information-interactive electrotactile sensory feedback scheme based on a muscle spindle model for TENS. Additionally, we designed a closed-loop myoelectric prosthetic hand system that employs this feedback scheme to convey electrotactile sensations via four-channel electrical stimulation with varying frequencies and currents while avoiding interference from electrical stimulation artifacts. The system was evaluated in tests involving four participants.Experimental results demonstrated that the system could provide stable and reliable prosthetic hand control while utilizing electrical stimulation. Furthermore, it verified that the multidimensional information-interactive sensory feedback scheme could effectively convey angle and force information from different fingers of the prosthetic hand, enabling users to discern the state of the prosthetic hand as well as the shape, size, length, and hardness of contacted objects. In the future, we aim to explore richer and more intuitive tactile feedback through electrical stimulation to uncover further possibilities.

REFERENCES

[1] H. Song, T.-H. Hsieh, S. H. Yeon, T. Shu, M. Nawrot, C. F. Landis, G. N. Friedman, E. A. Israel, S. Gutierrez-Arango, M. J. Carty, L. E. Freed, and H. M. Herr, "Continuous neural control of a bionic limb restores biomimetic gait after amputation," *Nature Medicine*, vol. 30, no. 7, pp. 2010–2019, Jul. 2024.

[2] U. Proske and S. C. Gandevia, "The proprioceptive senses: Their roles in signaling body shape, body position and movement, and muscle force," *Physiological Reviews*, vol. 92, no. 4, pp. 1651–1697, Oct. 2012.

[3] D. W. Tan, M. A. Schiefer, M. W. Keith, J. R. Anderson, J. Tyler, and D. J. Tyler, "A neural interface provides long-term stable natural touch perception," *Science Translational Medicine*, vol. 6, no. 257, pp. 257ra138–257ra138, Oct. 2014.

[4] E. A. Biddiss and T. T. Chau, "Upper limb prosthesis use and abandonment: A survey of the last 25 years," *Prosthetics and Orthotics International*, vol. 31, no. 3, p. 236, Sep. 2007.

[5] S. M. Engdahl, B. P. Christie, B. Kelly, A. Davis, C. A. Chestek, and D. H. Gates, "Surveying the interest of individuals with upper limb loss in novel prosthetic control techniques," *Journal of NeuroEngineering and Rehabilitation*, vol. 12, no. 1, p. 53, Jun. 2015.

[6] S. Raspopovic, M. Capogrosso, F. M. Petrini, M. Bonizzato, J. Rigosa, G. Di Pino, J. Carpaneto, M. Controzzi, T. Boretius, E. Fernandez, G. Granata, C. M. Oddo, L. Citi, A. L. Ciancio, C. Cipriani, M. C. Carrozza, W. Jensen, E. Guglielmelli, T. Stieglitz, P. M. Rossini, and S. Micera, "Restoring natural sensory feedback in real-time bidirectional hand prostheses," *Science Translational Medicine*, vol. 6, no. 222, pp. 222ra19–222ra19, Feb. 2014.

[7] M. Atzori, A. Gijsberts, C. Castellini, B. Caputo, A.-G. M. Hager, S. Elsig, G. Giatsidis, F. Bassetto, and H. Müller, "Electromyography data for non-invasive naturally-controlled robotic hand prostheses," *Scientific Data*, vol. 1, no. 1, p. 140053, Dec. 2014.

[8] D. J. Weber, M. Hao, M. A. Urbin, C. Schoenewald, and N. Lan, "Chapter twenty one - sensory information feedback for neural prostheses," in *Biomedical Information Technology (Second Edition)*, ser. Biomedical Engineering, D. D. Feng, Ed. Academic Press, Jan. 2020, pp. 687–715.

[9] C. Pandarinath and S. J. Bensmaia, "The science and engineering behind sensitized brain-controlled bionic hands," *Physiological Reviews*, vol. 102, no. 2, pp. 551–604, Apr. 2022.

[10] P. Svensson, U. Wijk, A. Björkman, and C. Antfolk, "A review of invasive and non-invasive sensory feedback in upper limb prostheses," *Expert Review of Medical Devices*, vol. 14, no. 6, pp. 439–447, Jun. 2017.

[11] V. Mendez, F. Iberite, S. Shokur, and S. Micera, "Current solutions and future trends for robotic prosthetic hands," *Annual Review of Control, Robotics, and Autonomous Systems*, vol. 4, no. Volume 4, 2021, pp. 595–627, May 2021.

[12] E. D'Anna, G. Valle, A. Mazzoni, I. Strauss, F. Iberite, J. Patton, F. M. Petrini, S. Raspopovic, G. Granata, R. Di Iorio, M. Controzzi, C. Cipriani, T. Stieglitz, P. M. Rossini, and S. Micera, "A closed-loop hand prosthesis with simultaneous intraneural tactile and position feedback," *Science Robotics*, vol. 4, no. 27, p. eaau8892, Feb. 2019.

[13] B. Stephens-Fripp, G. Alici, and R. Mutlu, "A review of non-invasive sensory feedback methods for transradial prosthetic hands," *IEEE Access*, vol. 6, pp. 6878–6899, 2018.

[14] M. A. Garenfeld, N. Jorgovanovic, V. Ilic, M. Strbac, M. Isakovic, J. L. Dideriksen, and S. Dosen, "A compact system for simultaneous stimulation and recording for closed-loop myoelectric control," *Journal of NeuroEngineering and Rehabilitation*, vol. 18, no. 1, p. 87, May 2021.

[15] E. D'Anna, F. M. Petrini, F. Artoni, I. Popovic, I. Simanić, S. Raspopovic, and S. Micera, "A somatotopic bidirectional hand prosthesis with transcutaneous electrical nerve stimulation based sensory feedback," *Scientific Reports*, vol. 7, no. 1, p. 10930, Sep. 2017.

[16] T. Rudjord, "A second order mechanical model of muscle spindle primary endings," *Kybernetik*, vol. 6, no. 6, pp. 205–213, Feb. 1970.

[17] Q. Ding, C. Tong, D. Liu, B. Yan, F. Wang, and S. Han, "Muscle spindle model-based non-invasive electrical stimulation for motion perception feedback in prosthetic hands," *IEEE Transactions on Neural Systems and Rehabilitation Engineering*, vol. 33, pp. 1316–1327, 2025.

[18] C. Qingzheng, T. Qing, Z. Muchao, and M. Luyao, "CNN-based gesture recognition using raw numerical gray-scale images of surface electromyography," *Biomedical Signal Processing and Control*, vol. 101, p. 107176, Mar. 2025.

[19] S. Dosen, M.-C. Schaeffer, and D. Farina, "Time-division multiplexing for myoelectric closed-loop control using electrotactile feedback," *Journal of Neuroengineering and Rehabilitation*, vol. 11, p. 138, Sep. 2014.

[20] D. Xiong, D. Zhang, X. Zhao, and Y. Zhao, "Deep learning for EMG-based human-machine interaction: A review," *IEEE/CAA Journal of Automatica Sinica*, vol. 8, no. 3, pp. 512–533, Mar. 2021.

[21] J. Zhang, C.-H. Chou, M. Hao, W. Liang, Z. Zhang, A. Xie, J. L. Patton, W. Pei, and N. Lan, "Somatotopically evoked tactile sensation via transcutaneous electrical nerve stimulation improves prosthetic sensorimotor performance," *IEEE Transactions on Neural Systems and Rehabilitation Engineering*, vol. 32, pp. 2815–2825, 2024.

[22] W. Liang, C. Qin, A. Sun, X. Zhang, N. Lan, and S. Bi, "Study of tactile sensation somatotopy and homology between projected fingers in residual limb and natural fingers in intact limb," *IEEE Transactions on Neural Systems and Rehabilitation Engineering*, vol. 31, pp. 636–645, 2023.

[23] J. A. George, D. T. Kluger, T. S. Davis, S. M. Wendelken, E. V. Okorokova, Q. He, C. C. Duncan, D. T. Hutchinson, Z. C. Thumser, D. T. Beckler, P. D. Marasco, S. J. Bensmaia, and G. A. Clark, "Biomimetic sensory feedback through peripheral nerve stimulation improves dexterous use of a bionic hand," *Science Robotics*, vol. 4, no. 32, p. eaax2352, Jul. 2019.

[24] Zhenzhi. Ying, Xianyu. Zhang, Shihao. Li, Koki. Nakashima, Liming. Shu, and Naohiko. Sugita, "Real-time dexterous prosthesis hand control by decoding neural information based on EMG decomposition," in *2024 IEEE International Conference on Robotics and Automation (ICRA)*, May 2024, pp. 966–972.

[25] J. W. Simatupang, W. Wijaya, D. Tyler, and C. Mavridis, "Simulation analysis of equivalent circuit model of skin-electrode impedance for transcutaneous electrical stimulation," *Bulletin of Electrical Engineering and Informatics*, vol. 10, no. 4, pp. 1936–1943, Aug. 2021.